Immunobiology 230 (2025) 153085

Contents lists available at ScienceDirect

Immunobiology

journal homepage: www.elsevier.com/locate/imbio

Mitochondrial RNA/RIG-I promotes Caspase-1/GSDMD-mediated inflammation in sepsis-associated acute kidney injury

Jie Jiao [a], Xuan Fang [a], Lisha Ma [a], Ruiqin Shen [a], Dongmei Li [a], Hao Luo [a], Aiping Xu [a], Zhaojun Xia [b], Sheng Jin [c], YunXia Shao [d], Mengya Wang [a], Decui Shao [a,*]

[a] Laboratory of Cell Electrophysiology, Wannan Medical College, Anhui, China
[b] Electron Microscopy Center, Wannan Medical College, Anhui, China
[c] Department of Physiology, Hebei Medical University, Hebei, China
[d] The Second People's Hospital of Wuhu, Anhui, China.

ARTICLE INFO

Editor: Banu Bayram

Keywords:
Sepsis
Acute kidney injury
Mitochondrial RNA
RIG-I
Caspase-1

SUMMARY

Mitochondria play a decisive role in the pathological mechanisms of acute kidney injury (AKI). However, the specific mechanisms by which mitochondria regulate inflammation in AKI remain elusive. We aimed to investigate the role of mitochondrial RNA (mtRNA) and retinoic acid-inducible gene I (RIG-I) in sepsis-induced renal injury. To establish an AKI mouse model, intraperitoneal injection of lipopolysaccharide was used. Meanwhile, NRK-52E cells were treated with lipopolysaccharide, ATP, and Nigericin (LAN). Western blotting and immunohistochemistry analyses revealed an upregulation of RIG-I expression in AKI samples. Depolarization of mitochondrial membrane potential and elevation of cytoplasmic mtRNA were observed after LAN treatment. RNA immunoprecipitation demonstrated a direct binding interaction between mtRNA and RIG-I. Additionally, mtRNA was shown to induce mitochondrial membrane potential depolarization, an effect that could be mitigated by RIG-I knockdown. It was observed that Caspase-1 and ASC associating with RIG-I through co-immunoprecipitation. The mitochondrial damage induced by LAN, along with the upregulation of caspase-1, cleaved caspase-1, GSDMD, and cleaved GSDMD, were mitigated by the knockdown of RIG-I. Additionally, GSDMD knockout attenuates lipopolysaccharide-induced renal injury and reduces the level of IL-1β and TNF-α in murine models. Our research indicates that the pathological processes of AKI are driven by mtRNA/RIG-I-mediated Caspase-1/GSDMD, leading to inflammation.

1. Introduction

Acute kidney injury (AKI) is a common clinical condition, with mortality rates among patients necessitating dialysis reaching as high as 60–80 % (Aniort et al., 2019). Sepsis is the leading cause of AKI in intensive care units, and aside from dialysis, no definitive treatment exists (Rane et al., 2025). Sepsis-associated AKI (SA-AKI) has been illustrated to result from disruptions in energy metabolism. Energy metabolism in cellular is from mitochondria, which play a critical role in intracellular oxidative phosphorylation and ATP synthesis (Liu et al., 2024; Wang et al., 2022).

Renal tubular epithelial cells (RTECs) consume large amounts of ATP for transport and have a high mitochondrial content; under conditions of stress, such as mitochondrial metabolic changes, impaired mitochondrial biosynthesis, reactive oxygen species (ROS) overproduction, and calcium loading, severe and prolonged stress ultimately leads to RTECs death (Guo et al., 2024). Histological features of AKI include the absence of the brush border of typical RTECs, flattening and focal loss of RTECs, and inflammatory cell infiltration (Kim et al., 2020; Sun et al., 2022).

The DNA found in the mitochondria (mtDNA) is responsible for coding synthesis and oxidative phosphorylation proteins. Urine mtDNA levels were higher in IgAN patients. Furthermore, in living donor kidney transplant patients, elevated plasma mtDNA levels correlate with transplant outcomes (Kroneisl et al., 2023; Yu et al., 2019). Damaged mtDNA is released into the cytoplasm during AKI through the mitochondrial membrane's Bax pores. Cytosolic mtDNA activates the cGAS-STING pathway, which then results in tubule inflammation (Huang et al., 2025; Maekawa et al., 2019). Leakage of cytoplasmic mtDNA inevitably occurs with mitochondrial RNA (mtRNA) spill, cytoplasmic acivated RNA sensors retinoic acid-inducible gene I (RIG-I) (Dhillon

* Corresponding author.
E-mail address: shaodecui@wnmc.edu.cn (D. Shao).

https://doi.org/10.1016/j.imbio.2025.153085
Received 27 January 2025; Received in revised form 28 May 2025; Accepted 3 June 2025
Available online 4 June 2025

et al., 2023; Dhir et al., 2018). However, the relationship between mtRNA and RIG-I in SA-AKI remains unclear.

RIG-I, encoded by DDx58, has been previously studied in viral infectious diseases. RIG-I is in a self-repression when resting. Upon exposure to double-stranded or single-stranded RNAs, RIG-I experiences a structural transformation, leading to the liberation of its caspase activation and recruitment domain (CARD). This release alleviates self-repression, allowing RIG-I can communicate with mitochondrial antiviral-signaling protein (MAVS), promoting interferon production and antiviral responses (Thoresen et al., 2021; Wicherska-Pawłowska et al., 2021). Recently, RIG-I has also received more attention for its role in non-infectious diseases. In atherosclerotic lesions, RIG-I is highly expressed, and targeting RIG-I inhibits inflammation (Wang et al., 2012). Family lines with lupus nephritis showed mutations in the DDx58 gene and DDx58 R109C mutation can deregulate the self-repression of the RIG-I protein and initiate the MAVS-mediated interferon-I signaling pathway leading to renal damage, suggests that RIG-I may represent a critical target for research in renal disease (Peng et al., 2023). Our previous research demonstrated that RIG-I contributes to chronic kidney disease progression through Caspase-1/GSDMD (Ma et al., 2023). However, it is unclear whether the RIG-I/Caspase-1/GSDMD contributes to SA-AKI inflammation. To address this, we established a SA-AKI mouse model to evaluate changes in mtRNA and RIG-I expression. Furthermore, we investigated whether mtRNA was involved in SA-AKI by regulating the RIG-I inflammasome in cultured RTECs.

2. Materials and methods

2.1. Establishment ofSA-AKI model

Shandong Experimental Animal Center supplied us with male C57BL/6 J mice. The Animal Welfare and Ethics Committee of Wannan Medical College have granted approvl for the conducted animal experiment (WNMC-AWE-2024024). To establish a SA-AKI model, animals were randomly divided into NS and lipopolysaccharide (LPS) groups. According to the literature, LPS (biosharp, BS904) with a dose of 10 mg/kg was injected intraperitoneally into mice for 16 h while saline was used as a control (Ren et al., 2020). Mice were randomly divided into four groups: WT, WT-LPS, GSDMD globally knockout ($GSDMD^{-/-}$), and $GSDMD^{-/-}$-LPS. The mice were euthanized using an injection of sodium pentobarbital (50 mg/kg). Blood and kidney samples were collected and stored at −80 °C for further analysis. Using a sodium pentobarbital injection (50 mg/kg), the mice were euthanized. Kidney samples were gathered and stored at −80 °C for subsequent analysis.

2.2. Transmission electron microscopy

The fresh mouse kidney tissue (1x2x3mm) was quickly placed in electron microscope fixative for at least 8 h. After washing with phosphate buffer solution (3 times, 10 min each time), it was fixed with 1 % osmium acid for 2 h. The kidney tissue was then washed with phosphate buffer solution (3 times, 10 min each time) and gradually dehydrated in alcohol solutions. Subsequently, the samples were placed in acetone and 812 embedding media. The samples were cut into 70-nm ultrathin sections using an ultramicrotome (RMC PT-PC LN Ultra). Lead and uranium were used to stain the sections. Observations and image analysis were performed via transmission electron microscopy (TEM) (Ht7800, HITACHI, Japan).

2.3. Human kidney sample

An Ethics Committee of Wuhu Second People's Hospital approved kidney biopsy samples from patients suffering from acute kidney injury, and all participants gave their consent orally or in writing (2024-KY-122).

2.4. Immunohistochemical examination

We used a primary anti-RIG-I antibody (invitrogen, 700,366) for immunohistochemical analysis, following the steps described in the literature (Yu et al., 2022).

2.5. Cell culture

Procell Life Sciences Technology Company provides renal tubular epithelial cells (NRK-52E). NRK-52E cells were cultured in DMEM (Gibco, C11995500BT), medium containing 10 % fetal bovine serum (TIANHANG, 80230–6412). Place the cells in a culture medium comprising 0.5 % fetal bovine serum overnight before processing. Initially, stimulate cells with 500 ng/mL LPS (sigma, 0111:B4) for 4 h, followed by 3 mM ATP (sigma, A2383) and 10 mM Nigericin (Invivogene, 28,643–80-3) for 1 h (Lin et al., 2020).

2.6. Western blotting

RIPA (Beyotime, P0013B, China) was used to obtain protein. We separated protein by 8 % -12 % SDS-PAGE and transferred it to PVDF membranes. After blocking with 5 % skim milk, PVDF membranes were incubated with specific primary antibodies that recognized RIG-I (3743, Cell Signaling Technology, USA), IL-1β (GTX74034, Gene Tex), Gasdermin D (39,754, Cell Signaling Technology, USA), Tom20 (YT4696, Immunoway), Cleaved-gasdermin D (10,137, Cell Signaling Technology, USA), NGAL (ab216462, abcam), Caspase-1 (24,232, Cell Signaling Technology, USA),Cleaved-caspase-1 (89,332, Cell Signaling Technology, USA), NLRP3 (A5652, Abclonal), IL-1β (12,507, Cell Signaling Technology, USA), Caspase-1 (A0964, Abclonal), Cleaved-caspase-1 (AF4005, Affinity). Following TBST washing, the second antibody was incubated at room temperature the following day. The ECL luminescent solution was proportionally configured, the strips were placed in the developer, and the luminescent solution was evenly spread on the protein surface of the strips for exposure. We analyze the grey values of the protein bands and normalize them with GAPDH.

2.7. Quantitative RT–PCR

A total RNA extract of tubular cells or kidney cortex samples was extracted and PCR was performed as we previous described (Ma et al., 2023). The corresponding primer sequences are list as following: Forword: ACCCATCACCATCTTCCAGGAG, Reverse: GACATACTCAG CACCAGCATCAC for GAPDH; Forward AGCCACATCAAGTCT TTCAGTCTAC, Reverse:AGGAGGACGGATAAGAGGATAATGG for Nd1; Forward: ACACGATGAGGCAACCAAACAG, Reverse:AATGAGGGCAAT-TAAGAGTGGGATG for Nd4; Forward: CGAATGAATCTGAGGAGGC TTCTC, Reverse: CGGCGATAATGAATGGGAGGATG for Cytb.

2.8. Mitochondrial membrane potential measurement

JC-1 assay kit (C200, Beyotime, China) is used to determine mitochondrial membrane potential. Stain the cells with JC-1 staining solution (250 uL, 37 °C, incubate for 20 min); Following the removal of the JC-1 staining solution, perform two washes using the staining wash solution. Subsequently, add 200 μL of fresh culture medium and proceed to observe the specimen under a fluorescent microscope.

2.9. Mitochondrial isolation

Use a commercially available mitochondrial separation reagent kit (Beyotime, shanghai, China). First, wash the cells with PBS, then add the mitochondrial separation reagent (2 mL, ice-bath, incubate for 15 min). The cell suspension was homogenized 10–30 times in a glass homogenizer (1000 g for 10 min at 4 °C). Subsequently, the supernatant was collected and centrifuged at 3500*g* for 10 min at 4 °C. At this time, the

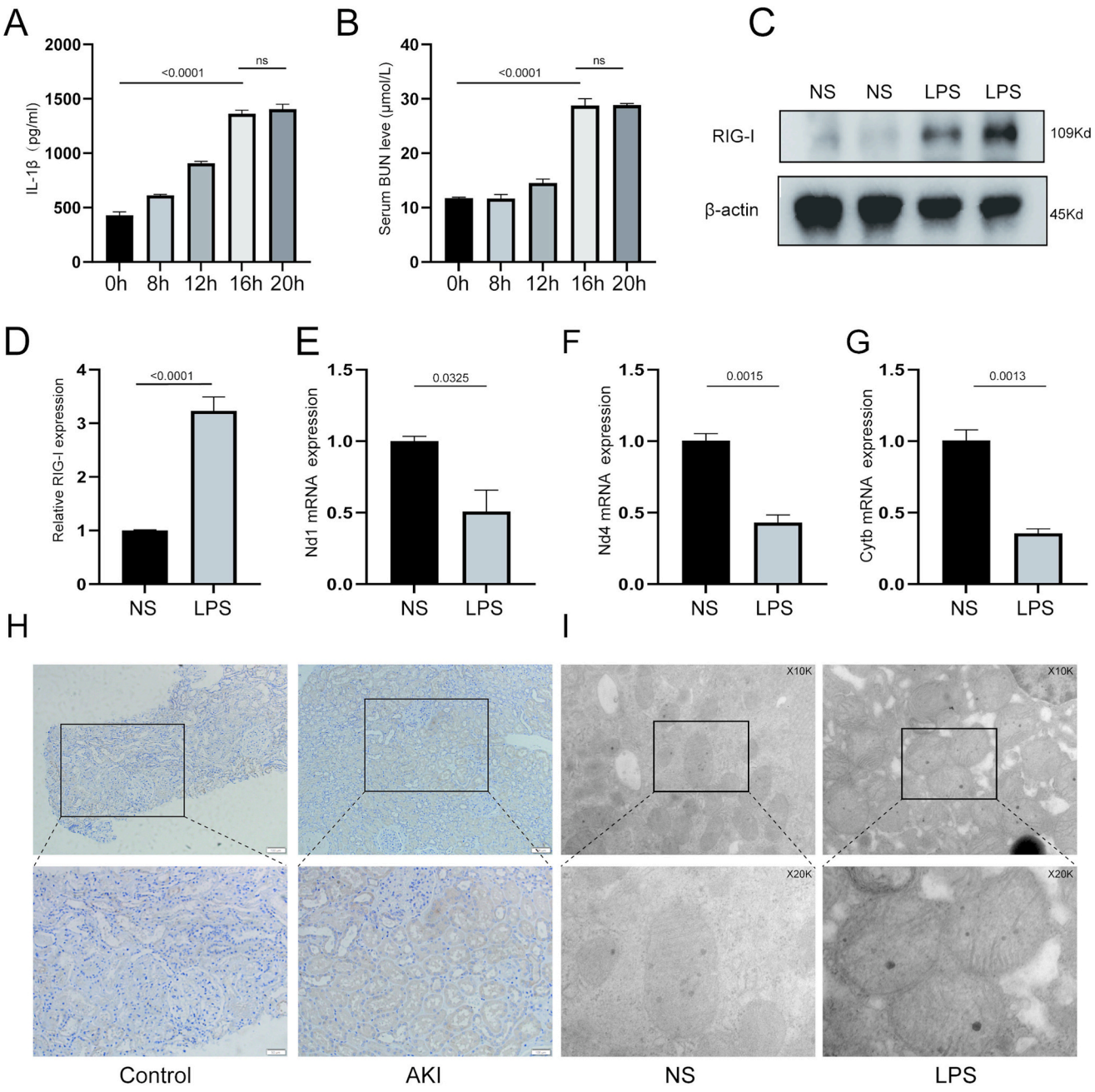

(caption on next page)

Fig. 1. The effect of LPS on RIG-I expression and mitochondrial damage in mice; (A) ELISA results showed the changes of IL-1β in renal tissue after LPS treatment with different time gradients ($n = 3$); (B)The results of blood urea nitrogen showed the changes of serum urea nitrogen content in different time gradients (n = 3); (C—D)Western blot showed that the protein level of RIG-I in the renal tissue of LPS-treated mice were significantly elevated ($n = 5$); (*E*-G)The LPS-induced in vivo model reduced mRNA levels of Nd1 (n = 3), Nd4 ($n = 4$), and Cytb (n = 4); (H)AKI kidney tissue immunohistochemistry showed that RIG-I expression was high in renal tubules; (I)Mice with normal and LPS renal tissue showed differences in mitochondrial morphology using transmission electron microscopy; (J) A cluster heatmap of associated proteins in AKI (n = 5) was generated, with colour gradients ranging from blue (decreased expression) to white (low intensity) to red (increased expression). (For interpretation of the references to colour in this figure legend, the reader is referred to the web version of this article.)

precipitate was the isolated mitochondria, and the supernatant was the cytoplasm from which the mitochondria had been removed.

2.10. Co-immunoprecipitation

Using RIPA lysis buffer, extract total protein. Combine 1 μg of RIG-I antibody with 30 mL of Protein-A/G agarose (Ca#20421, Thermo Fisher Scientific, USA) and shake well overnight. Immunoblot analysis was performed using RIG-I, Caspase-1, and ASC antibodies.

2.11. RNA immunoprecipitation

Using the RNA immunoprecipitation (RIP) kit (Ca#Bes5101, BersinBio, China), cells in the NC and LAN treatment groups were lysed using the kit's own lysis buffer. RIG-I antibody (5 μg) or control IgG were used to incubate the cells. Cell lysis buffer was added overnight at 4 °C. Subsequently, Protein A/G magnetic beads are combined and shaken at 4 °C for 1 h. From the lysis buffer, total RNA was extracted. Analysis of mitochondrial-specific genes Nd1, Nd4, and Cytb was performed using quantitative RT-PCR. The mtRNA enrichment in RIG-I antibody relative to control IgG was calculated as fold.

2.12. RNA interference

NRK-52E was transfected with siRNA (50 nmol/L) by transfection kit (C10511–05, RiboBio, China). The siRNAs utilized have the following sequences: RIG-I siRNA: CCATGCTGCACATCTGCAA; NLRP3 siRNA: GGAGTCACTGTTATGAGAT; Caspase-1 siRNA: GGGCAAGCCAGATGTTTAT; GSDMD siRNA: GTCAAGTCTAGGCCAGAAA.

2.13. ELISA assay

According to our previous literature, IL-1β level in kidney was detected using the ELISA assay kit (Dako Bioengineering, Shenzhen, China).

2.14. Proteins enrichment by acetone

The cell incubation solution was thoroughly mixed with pre-cooled acetone at 1:4 and placed at −20 °C overnight. The next day, after centrifugation at 12000 rpm for 15–30 min at 4 °C, the supernatant was discarded from the samples, and the acetone was allowed to fully volatilize the remaining protein precipitate for the next IL-1β protein detection.

2.15. Statistical analysis

Data are presented as mean ± SEM. In this study, we used GraphPad Pris and ImageJ applications to draw bar charts and present the results using Adobe illustrator. Comparisons between two groups were carried out using the *t*-test; the differences among multiple groups were analyzed using one-way ANOVAs, which were considered significant when $P < 0.05$ was used.

3. Results

3.1. LPS treatment leads to mitochondrial damage and increased RIG-I expression

LPS treatment time gradient showed that serum IL-1β and serum urea nitrogen content reached the peak at 16 h after LPS injection (Fig. 1 A-B).A significant increase in RIG-I protein level was detected in the kidney cortex of LPS-treated mice (Fig. 1 C—D).Real-time qPCR showed that LPS lessened mitochondrial-specific genes (Nd1, Nd4, Cytb) levels in kidney tissue (Fig. 1E-G). In human clinical samples, immunohistochemistry revealed RIG-I deposition in renal tubules of paracancerous control tissues. However, in AKI specimens, significantly stronger RIG-I deposition was observed specifically in injured tubules, with no no obvious deposition in glomeruli (Fig. 1H). Transmission electron microscopy revealed mitochondrial swelling and a decreased aspect ratio (long axis/short axis) in renal tissue in the LPS-induced mice (Fig. 1 I). The Gene Expression Omnibus (GEO, GSE240304)) was utilized to analyze gene expression profiles in an AKI mouse model, revealing significant upregulation of pyroptosis-related genes, inflammatory mediators, and pattern recognition receptors, including DDX58, NLRP3, and AIM2.Meanwhile, mitochondrial-related gene expression was notably downregulated in AKI mice (Fig. 1J).

3.2. MtRNA releasing activates RIG-I

To assess mitochondrial membrane potential, the mitochondrial fluorescence probe JC-1 was employed. The green fluorescence increased in NRK-52E after LPS, ATP, and Nigericin (LAN) treatment, indicating depolarization of mitochondrial membrane potential (Fig. 2A). To evaluate the changes in cytoplasmic mtRNA response to LAN in NRK-52E, we isolated cytoplasmic components from NRK-52E and extracted RNA. Analysis confirmed no significant mitochondrial contamination in the cytoplasmic components, as evidenced by the presence of GAPDH and the absence of Tom20 (mitochondria) (Fig. 2B). Real-time qPCR of mitochondrial-specific genes Nd1, Nd4, and Cytb showed that after LAN treatment, the transcription level of the cytoplasmic part was higher (Fig. 2C-E).RIG-I antibody group showed increased enrichment of genes related to mtRNA (Nd1, Nd4, Cytb) in comparison with control IgG group (Fig. 2F-H).

3.3. RIG-I inflammasome participates in LAN induced inflammatory response

RIG-I, Caspase-1, and ASC each contain CARD domains in their structures. Structural analysis indicates that RIG-I can indirectly interact with Caspase-1 and ASC through CARD-mediated mechanisms, while also exhibiting the capacity for direct binding to Caspase-1 through its CARD domain (Fig. 3A-B).Following LPS treatment, the expression levels of RIG-I and ASC proteins in immunoprecipitated NRK-52E cells were elevated. Moreover, co-immunoprecipitation assays demonstrated that RIG-I physically binds to both ASC and Caspase-1 (Fig. 3C).

Western blot analysis displayed RNA interference targeting NLRP3 and RIG-I significantly attenuated the upregulated protein expression of NLRP3 and RIG-I induced by LAN (Fig. 4A-B). Similarly, RNA interference directed against Caspase-1 and GSDMD effectively suppressed the LAN-induced elevation in Caspase-1 and GSDMD protein expression (Fig. 4C-D). Furthermore, the LAN-induced elevation in Cleaved-

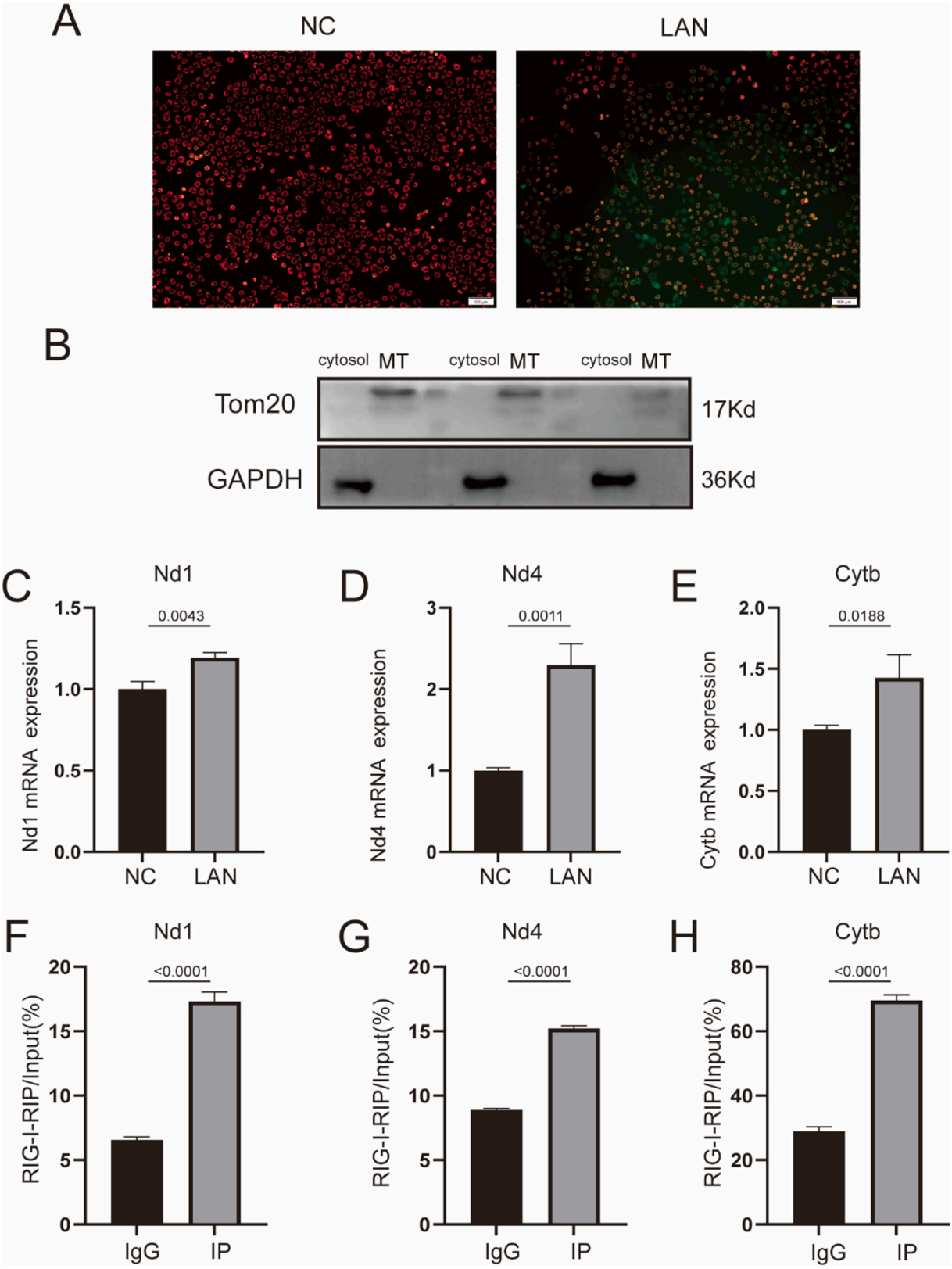

Fig. 2. Release of mtRNA into the cytoplasm activates RIG-I; (A)JC-1 results showed that LAN treatment caused depolarization of mitochondrial membrane potential in NRK-52E cells; (B)Western blot verified the separation efficiency of mitochondria (MT) and cytoplasm; Tom20: mitochondrial membrane marker; (C-E)qPCR results showed that the mRNA level of Nd1 (n = 3), Nd4 (n = 3) and Cytb (n = 3) in the cytoplasm increased after LAN-treatment; (F—H)The results of RIP analysis revealed RIG-I directly senses mtRNA (n = 4) in NRK-52E cells after LAN treatment.

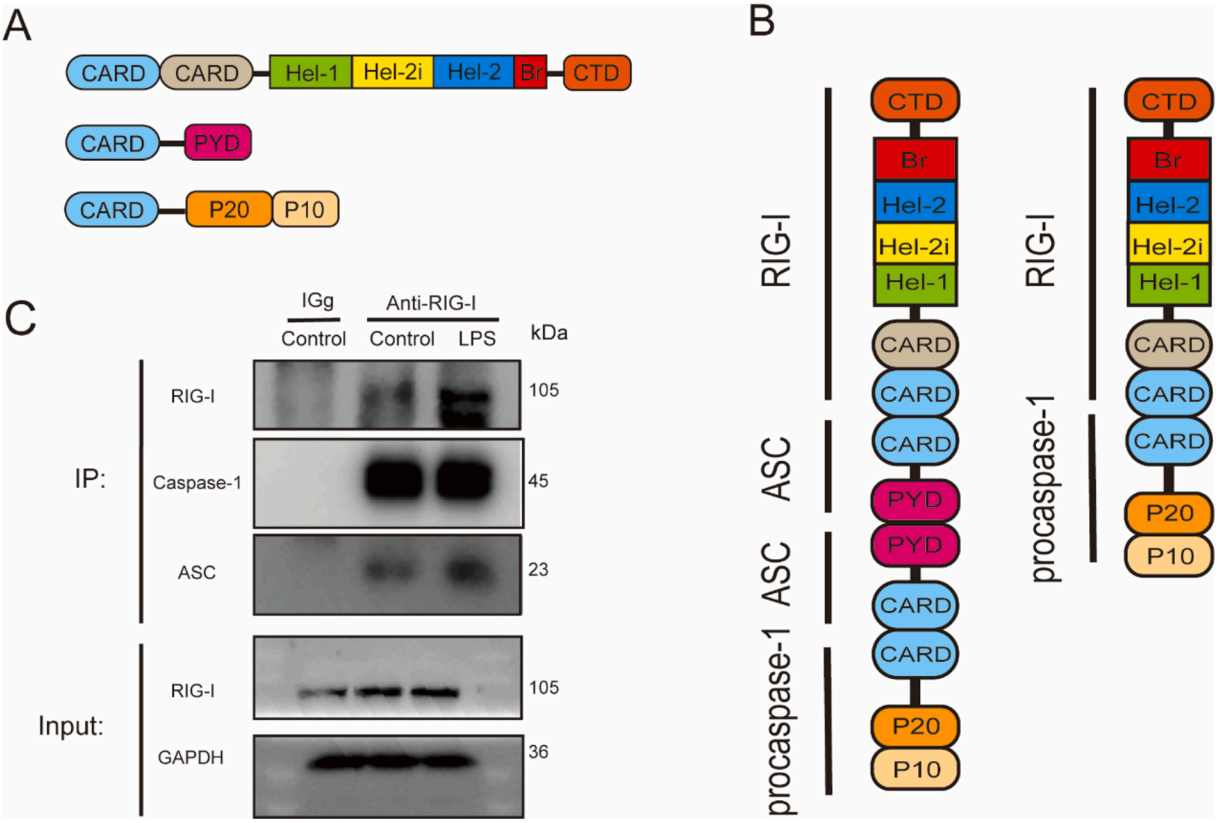

Fig. 3. Co-IP showed that RIG-I binds to ASC and Caspase-1; (A)Diagram of the molecular structure of RIG-I, Caspase-1, and ASC; (B)Model prediction for RIG-I and Caspase-1, as well as RIG-I, ASC and Caspase-1; (C)The results of Co-IP analysis revealed interactions between RIG-I and Caspase-1, RIG-I and ASC in LAN-treated NRK-52E cells.

Caspase-1, Caspase-1, and IL-1β levels was inhibited by NLRP3 RNA interference, with the combined knockdown of NLRP3 and RIG-I exhibiting a more pronounced inhibitory effect compared to NLRP3 knockdown alone (Fig. 4E-G).

3.4. RIG-I/Capase-1/GSDMD participates in LAN induced inflammatory response

After LAN administration, Western blot showed increased protein levels of Caspase-1, Cleaved-Caspase-1, GSDMD, Cleaved-GSDMD, and IL-1β. These elevations were reversed by siRNA targeting RIG-I (Fig. 5A-F).

The upregulation of cleaved-Caspase-1, GSDMD and IL-1β protein level induced by LAN was significantly mitigated by siRNA-Caspase-1 (Fig. 5G-J). Furthermore, LAN treatment resulted in elevated levels of cleaved-GSDMD and IL-1β protein levels, an effect that was effectively suppressed by siRNA targeting GSDMD (Fig. 5K-L). JC-1 fluorescence analysis showed that mtRNA and LAN treatment significantly increased depolarization of mitochondrial membrane potential. Notably, this depolarization was alleviated following the application of siRNA targeting RIG-I (Fig. 6A-D).

3.5. GSDMD knockout are resistant to kidney damage in SA-AKI mice

Histopathological examination using H&E staining identified distinct tubular epithelial alterations in the SA-AKI mice, with prominent vacuolar degeneration particularly evident in proximal tubular segments (arrowheads). In contrast, renal tissue sections from LPS-challenged GSDMD-deficient mice maintained normal tubular architecture without detectable pathological changes(Fig. 7A).GSDMD knockout mice demonstrated lower levels of serum creatinine and blood urea nitrogen after LPS treatment than wild-type mice (Fig. 7B-C). In addition, IL-1β and TNF-α levels were significantly increased after LPS treatment, as determined by ELISA, and this effect was alleviated in GSDMD knockout mice (Fig. 7D-E). Protein expression levels of IL-1β increased in wild-type mice after LPS injection, but this increase was attenuated by GSDMD knockout. Protein expression levels of NGAL, a marker of AKI, were notably lower in GSDMD knockout mice compared to wild-type mice (Fig. 7F-L).

4. Discussion

RIG-I functions as a pattern recognition receptor with an evolving role that extends beyond its initial identification of viral RNA/DNA and activation of antiviral immune responses. It now plays a crucial role in regulating various pathological and physiological processes across different diseases. Nevertheless, the specific role and underlying mechanisms of the RIG-I-mediated inflammatory response in the context of SA-AKI remain inadequately understood. In this research, we discovered that cytoplasmic mtRNA increased following AKI, and that mtRNA serves as an activator of RIG-I. Subsequently, ASC and Caspase-1 combined with RIG-I to create inflammasome complexes, leading to NLRP3-independent pyroptosis. Knockdown of RIG-I attenuates LAN-induced pyroptosis and inflammatory responses in RTECs.

The stimulation of RIG-I in cardiac fibroblasts increases the production of pro-inflammatory cytokines, including IL-6 and IL-8, leading to heart damage and cardiomyopathy (Li et al., 2021). Within the hematopoietic system, RIG-I has been identified as a critical negative regulator of myelopoiesis, with its expression levels dynamically increasing during bone marrow differentiation (Zhang et al., 2008). RIG-I exhibits a dual, context-dependent role in liver pathophysiology. In nonalcoholic steatohepatitis, hepatic RIG-I expression is markedly

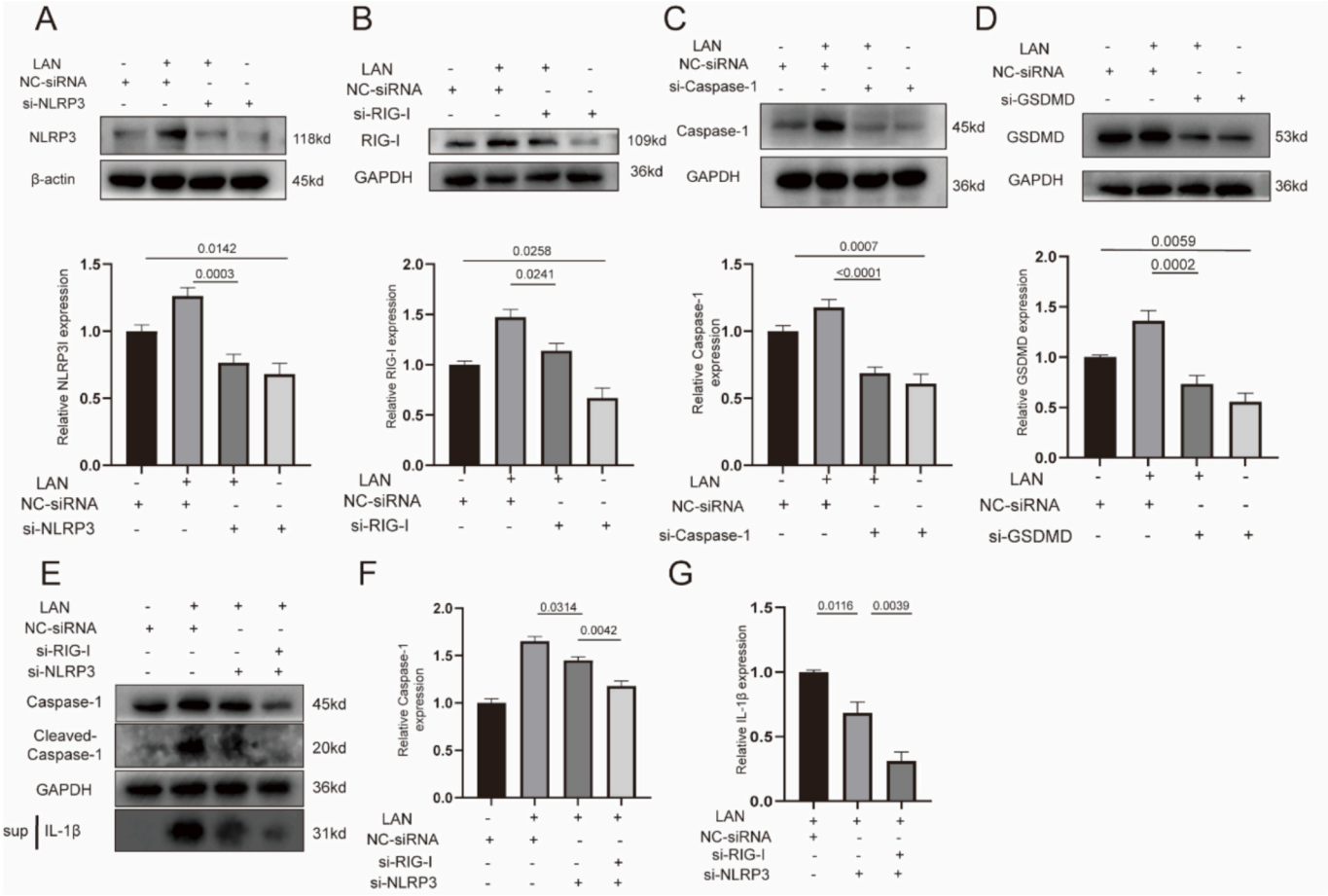

Fig. 4. RIG-I inflammasome participates in LAN induced inflammatory response; (A-F)Western blot showed the knockdown efficiency of siNLRP3 (n = 5), siRIG-I (*n* = 6), siCaspase-1 (n = 5) and siGSDMD (n = 5); (E-G)Western blot was used to analysis the effect of siNLRP3/ siRIG-I co-knockdown on Caspase-1 (n = 5) and IL-1β (n = 5).

reduced. Notably, RIG-I deficiency exacerbates hepatocyte apoptosis, while its overexpression confers protection against palmitate-induced cytotoxicity through autophagy induction (Frietze et al., 2022). However, this protective mechanism contrasts with its role in metabolic dysfunction-associated steatotic liver disease, where hepatocyte-specific RIG-I knockout actually improves high-fat diet-induced glucose intolerance, insulin resistance, and hepatic steatosis (Seok et al., 2024). Intriguingly, RIG-I also demonstrates cell-type-specific dual functions in immunity. In alveolar macrophages, it potentiates antiviral defense by activating SREBP1-dependent noncanonical type I interferon signaling during cholesterol metabolism modulation (Nishimura et al., 2025) Conversely, in tumor-infiltrating $CD8^+$ T cells, RIG-I acts as an intracellular immunosuppressive checkpoint that limits $CD8^+$ T cell function and antitumor immunity (Duan et al., 2024). In our study, we indicate that inhibition of RIG-I may attenuate renal tubular injury in AKI.

The kidney is a highly metabolically active organ, characterized by an abundance of mitochondria, especially the proximal tubules of the kidney, which require a large amount of ATP to maintain their reabsorptive and secretory functions. Serving both as a primary source of cellular energy and as crucial regulators of cell death mechanisms, mitochondria are also acknowledged as essential contributors to AKI (Yao et al., 2024; Zhang et al., 2021). ATP imaging has revealed that cisplatin treatment and ischemia-reperfusion events decrease ATP levels within proximal tubules of GO-ATeam2 mice (Yamamoto et al., 2024). In addition, alterations in the structure of mitochondria lead to the activation of permeability transition pores, which facilitating the release of pro-apoptotic agents such as cytochrome C, thereby promoting apoptosis in renal cells (Li et al., 2024). In this study, we observed that the mice treated with LPS showed signs of mitochondrial swelling, a decrease in the average aspect ratio (long/short axis), and an increase in inflammatory factors. In addition to LPS-associated AKI, other forms of AKI also require investigation. Gene expression analysis revealed upregulated inflammatory factors and downregulated mitochondrial-related genes in cisplatin-induced AKI. The LPS model is widely used for SA-AKI research due to its similarity to human sepsis. LPS, a component of Gram-negative bacteria, interacts with pattern recognition receptors, such as Toll-like receptors (TLR2 and TLR4) on RTECs, triggering the release of pro-inflammatory cytokines and chemokines(Castellano et al., 2019; Dou et al., 2022). This inflammatory response leads to RTECs apoptosis and necrosis, causing renal dysfunction. Cisplatin, a key cancer drug, causes nephrotoxicity mainly through the organic cation transporter 2 on renal proximal tubular cells, which facilitates cisplatin uptake (Shin et al., 2023). Although LPS and cisplatin induce kidney injury through distinct molecular mechanisms, both can elicit inflammatory responses and cell death in renal tubular epithelial cells. However, whether the RIG-I signaling pathway contributes to cisplatin or other injury mediated renal tubular damage need future studies.

In the process of mitochondrial regulation of inflammation, mitochondria are regarded as evolutionary remnants of alphaproteobacteria, and some components of mitochondria are highly similar to bacterial molecules (Muñoz-Gómez et al., 2017), suggesting that these components can serve as ligands for pattern recognition receptors. Mitochondria contain unique circular double-stranded DNA, called mtDNA, which also encodes proteins essential for transcription and translation into proteins to produce energy-carrying ATP molecules. Under stress, mtDNA acts as damage-associated molecular patterns, released from

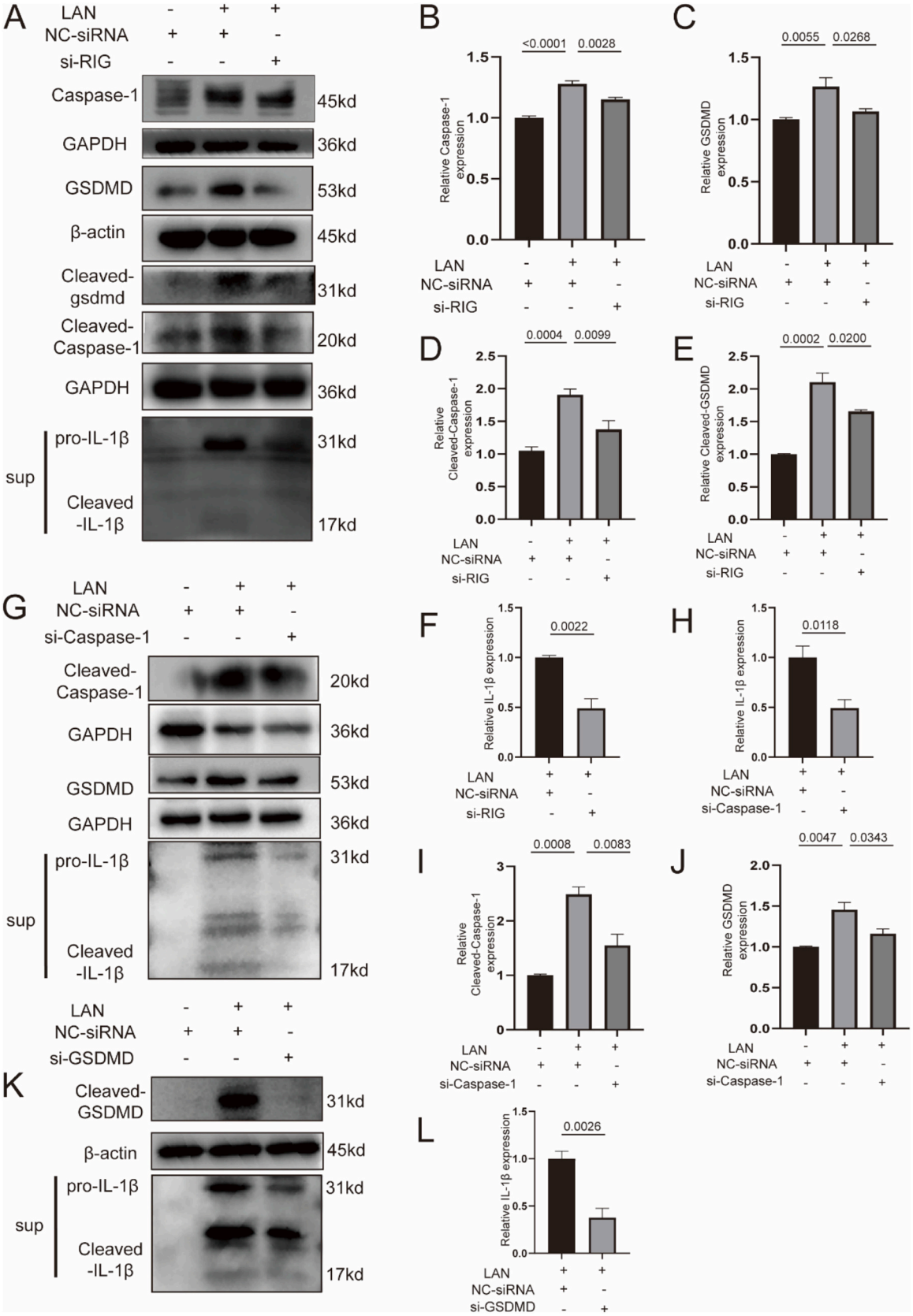

Fig. 5. Activation of RIG-I/Caspase-1/GSDMD signal in LAN-treated NRK-52E; (A-F)Western blot showed siRIG-I alleviated the expression of pyroptosis-related proteins Caspase-1 (n = 4), Cleaved-Caspase-1 (n = 4), GSDMD (n = 4), Cleaved-GSDMD (n = 3) and the release of IL-1β (n = 4) caused by LAN; (G-J)Western blot showed siCaspase-1 alleviated LAN-induced pyroptosis-related protein cleave-Caspase-1 (n = 3) and GSDMD (n = 3) expression and pro-IL-1β (n = 4) release; (K-L)Western blot showed siGSDMD alleviate LAN-induced pyroptosis-related protein GSDMD expression and pro-IL-1β (n = 4).

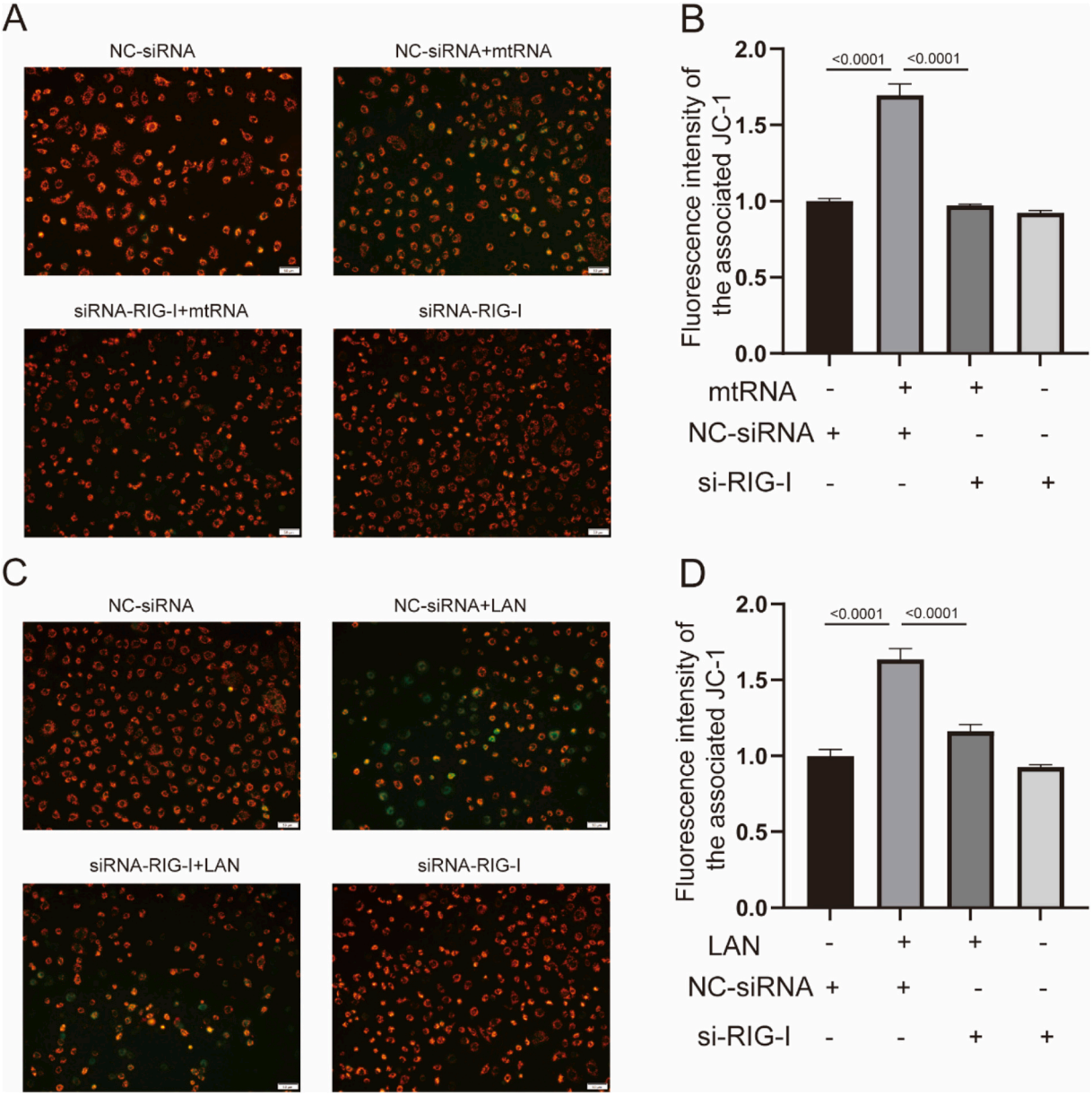

Fig. 6. RIG-I knockdown alleviated the mitochondrial membrane potential depolarization caused by mtRNA or LAN; (A-B)The JC-1 results showed that siRIG-I reduced the depolarization of mitochondrial membrane potential caused by mtRNA; (C—D)The JC-1 results showed that siRIG-I reduced the depolarization of mitochondrial membrane potential caused by LAN.

membrane pores formed by mitochondrial Bax/Bak1 into the cytoplasm, and then activate cGAS-STING to drive inflammatory response in AKI mice (Maekawa et al., 2019). The release of mtDNA will invariably accompanied by the leakage of mtRNA. The release of mtRNA into the cytoplasm activates RIG-I, which is also involved in mitochondrial control of inflammation (Marchi et al., 2023). In ischemia/reperfusion-induced kidney injury, cGAS deficiency mitigated inflammation and kidney damage (Li et al., 2024). RIG-I deficiency similarly reduced kidney injury from cisplatin (Doke et al., 2023). In our study, we identified a notable upregulation of RIG-I expression in SA-AKI. Furthermore, our observations indicated that LAN stimulation induced the release of mtRNA into the cytoplasm.We demonstrated that RIG-I binds to mtRNA, suggesting that the inflammatory response triggered by the mtRNA/RIG-I pathway participates in SA-AKI. The interaction between the mtRNA-RIG-I and mtDNA-GAS pathways and their roles in SA-AKI remain unclear and require further investigation.

LPS and ATP are conventional inflammasome activators, which activate the NLRP3. NLRP3 oligomerization induces caspase-1 activation, which subsequently catalyzes the proteolytic cleavage and release of key pro-inflammatory cytokines. These cytokines serve as critical drivers of renal inflammatory injury and contribute to the pathogenesis of multiple kidney diseases, including SA-AKI and environmental pollutant-induced kidney damage (Leventoğlu and Bakkaloğlu, 2024; Lu et al., 2024; Lu et al., 2022). In the present study, we observed that the reduction of NLRP3 expression attenuated the inflammatory response in RTECs induced by LAN. Notably, simultaneous knockdown of NLRP3 and RIG-I resulted in a more pronounced suppression of the LAN-induced inflammatory response compared to NLRP3 inhibition alone. These findings indicate that the inflammatory signaling triggered by LAN involves not only the NLRP3 inflammasome but also the RIG-I pathway.

As a critical component of the immune system, LPS treatment of endothelial cells can promote the transcription and translation of RIG-I (Imaizumi et al., 2002; Lin et al., 2020). RIG-I is a highly conserved

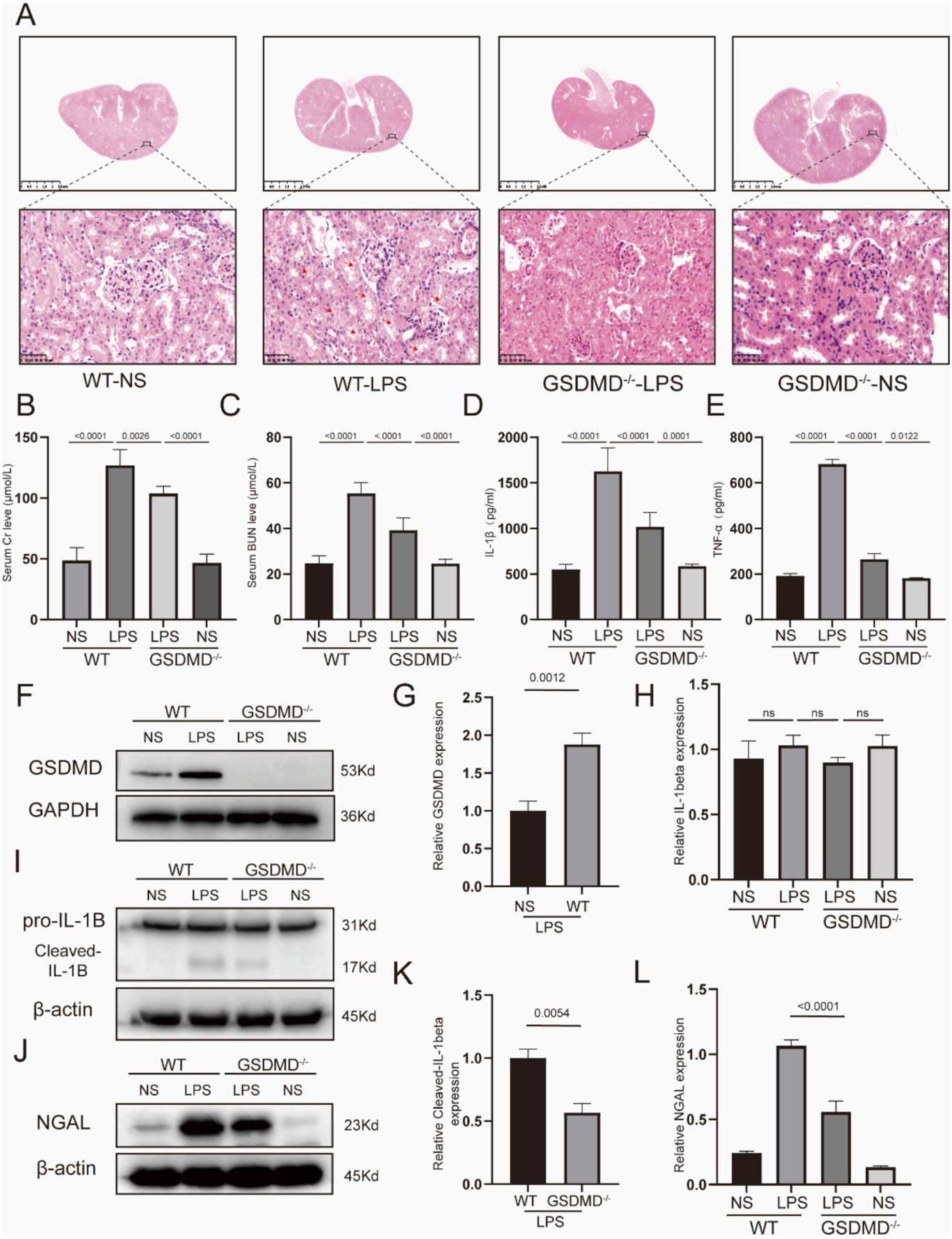

(caption on next page)

Fig. 7. GSDMD knockout alleviates LPS induced kidney injury in mice; (A)Representative images showing H&E staining of renal sections, vacuolization of renal tubules (red arrow, the scale bar of the magnified image is 50 uM); (B—C)Changes in SCr (n = 6) and BUN (n = 6) level in WT and GSDMD$^{-/-}$ groups with and without LPS treatment; (D-E) ELISA results showed the changes of IL-1β and TNF-α in renal tissue after LPS treatment in different groups (n = 6); (F-L)The protein expression of GSDMD (n = 5), IL-1β (n = 5), Cleaved-IL-1β (n = 4) and NGAL (n = 6) were detected by Western blot. (For interpretation of the references to colour in this figure legend, the reader is referred to the web version of this article.)

protein throughout evolution, comprising 925 amino acid residues in humans and organized into three distinct domains: the CARD domains, the central DECH box RNA helicase domain, and the C-terminal regulatory domain. The initiation of downstream signaling pathways is contingent upon the N-terminal CARD domain(Sikorska et al., 2023). Notably, Caspase-1 also possesses a CARD domain, with CARD-CARD interactions serving as the fundamental mechanism for RIG-I inflammasome assembly. It has been suggested that RIG-I is required for Caspase-1 activation and Cleaved IL-1β production triggered by VSV or 3prna (Poeck et al., 2010). Our prior research has demonstrated that in chronic kidney disease, the overexpression of RIG-I increases Caspase-1 activity and regulates the inflammatory response (Ma et al., 2023). In primary lung epithelial cells, RIG-I directly binds to Caspase-1 and ASC to promote IL-1β production (Pothlichet et al., 2013). The activation of the epithelial RIG-I inflammasome by rhinovirus suppresses antiviral immunity while facilitating virus-induced asthma exacerbations and inflammatory responses (Radzikowska et al., 2023). In the current study, we further confirmed the protein-level interaction between RIG-I and ASC, suggesting that RIG-I and ASC assemble into inflammasomes, activate Caspase-1, and confirm the role of RIG-I inflammasomes in SA-AKI. However, further experiments are needed to clarify which key CARD sites RIG-I regulate Caspase-1.

RTECs sustain damage and release a multitude of inflammatory factors and chemokines, initiating an inflammatory response. This inflammatory cascade recruits various immune cells, which exacerbate the inflammatory cascade. RTECs and immune cells jointly influence the disease progression through complex interactions in AKI (Gao et al., 2024). Single-cell RNA sequencing technology has been employed to analyze the renal transcriptome profile of kidney tissue from patients with ischemic-AKI. The results revealed significant enrichment of the RIG-I signaling pathway in proximal tubule cells, highlighting its critical role in the pathogenesis of AKI (Tang et al., 2023). In a folate-induced kidney injury model, inflammation and fibrosis were markedly reduced in the kidneys of RIG-I knockout mice (Dhillon et al., 2023). Additionally, in crush syndrome-induced AKI, RIG-I was found to promote macrophage polarization towards the M1 phenotype and induce macrophage pyroptosis. Knockdown of RIG-I expression reduced the expression of key molecules associated with M1 polarization (Li et al., 2022). These findings indicate that RIG-I in both macrophages and innate immune cells plays a pivotal role in driving the inflammatory and fibrotic responses in AKI.A limitation of our study is the absence of validation using macrophage or renal tubular epithelial cell-specific gene knockout mice, which would further clarify their distinct roles in the AKI.

Pyroptosis, initiated by inflammasomes and subsequently activated by Caspase-1 or Caspase-4/−5/−11, induced cell membrane rupture, and oligomerized activated GSDMD formed pores on the cell membrane to release cytokines, including IL-1β and IL-18(Li and Guo, 2025). Recently evidence suggests that GSDMD activation is a critical factor in the onset of cisplatin-associated AKI (Li et al., 2020). GSDMD knockout could significantly alleviate ischemia-reperfusion or cisplatin treatment induced renal damage (Miao et al., 2019). Serum GSDMD and Caspase-1 levels are elevated and GSDMD levels predict the prognosis of end-stage kidney disease patients (Zhang and Yang, 2024). Our current investigation also noted that knocking out the GSDMD gene alleviated LPS-related kidney injury. Numerous studies suggest that the suppression of pyroptosis may mitigate kidney injury; however, the specific roles of bone marrow-derived versus renal parenchymal cells in this process remain contentious (Islamuddin and Qin, 2024; Li et al., 2020; Miao et al., 2019). Given that our current research employs global knockout mice, the possibility that the attenuation of macrophage-derived pyroptosis contributes to reduced kidney damage cannot be excluded. To further elucidate this matter, future experiments will involve the use of mice with a GSDMD-specific knockout in renal tubular epithelial cells.

Our research suggests that RIG-I is cytoplasmic mtRNA sensor following mitochondrial injury. After RIG-I activation, the RIG-I inflammasome and its Caspase-1/GSDMD lead to the release of inflammatory cytokine IL-1β in tubular cell. Targeting signal molecules related to RIG-I and its pathways could serve as new targets for SA-AKI therapy.

CRediT authorship contribution statement

Jie Jiao: Investigation, Data curation, Conceptualization. **Xuan Fang:** Investigation. **Lisha Ma:** Formal analysis. **Ruiqin Shen:** Investigation. **Dongmei Li:** Investigation. **Hao Luo:** Funding acquisition. **Aiping Xu:** Supervision. **Zhaojun Xia:** Investigation. **Sheng Jin:** Supervision. **YunXia Shao:** Resources. **Mengya Wang:** Writing – review & editing. **Decui Shao:** Writing – review & editing, Writing – original draft, Conceptualization.

Funding

This work was supported by NSF of Higher Education Institutions (2022AH040173&2023AH051778&2022AH051245), Anhui Provincial NSF (1508085QH153) and NSF of China (81400695).

Declaration of competing interest

The authors declare that they have no known competing financial interests or personal relationships that could have appeared to influence the work reported in this paper.

Data availability

Data will be made available on request.

References

Aniort, J., Heng, A., Deteix, P., Souweine, B., Lautrette, A., 2019. Epidemiology of acute renal failure. Nephrologie Therapeutique 15, 63–69.
Castellano, G., Stasi, A., Franzin, R., Sallustio, F., Divella, C., Spinelli, A., Netti, G.S., Fiaccadori, E., Cantaluppi, V., Crovace, A., et al., 2019. LPS-binding protein modulates acute renal fibrosis by Inducing pericyte-to-myofibroblast trans-differentiation through TLR-4 signaling. Int. J. Mol. Sci. 20, 3682.
Dhillon, P., Mulholland, K.A., Hu, H., Park, J., Sheng, X., Abedini, A., Liu, H., Vassalotti, A., Wu, J., Susztak, K., 2023. Increased levels of endogenous retroviruses trigger fibroinflammation and play a role in kidney disease development. Nat. Commun. 14, 559.
Dhir, A., Dhir, S., Borowski, L.S., Jimenez, L., Teitell, M., Rötig, A., Crow, Y.J., Rice, G.I., Duffy, D., Tamby, C., et al., 2018. Mitochondrial double-stranded RNA triggers antiviral signalling in humans. Nature 560, 238–242.
Doke, T., Mukherjee, S., Mukhi, D., Dhillon, P., Abedini, A., Davis, J.G., Chellappa, K., Chen, B., Baur, J.A., Susztak, K., 2023. NAD(+) precursor supplementation prevents mtRNA/RIG-I-dependent inflammation during kidney injury. Nat. Metab. 5, 414–430.
Dou, X., Yan, D., Ma, Z., Gao, N., Shan, A., 2022. Sodium butyrate alleviates LPS-induced kidney injury via inhibiting TLR2/4 to regulate rBD2 expression. J. Food Biochem. 46, e14126.
Duan, X., Hu, J., Zhang, Y., Zhao, X., Yang, M., Sun, T., Liu, S., Chen, X., Feng, J., Li, W., et al., 2024. RIG-I is an intracellular checkpoint that limits CD8(+) T-cell antitumour immunity. EMBO Mol. Med. 16, 3005–3025.
Frietze, K.K., Brown, A.M., Das, D., Franks, R.G., Cunningham, J.L., Hayward, M., Nickels Jr., J.T., 2022. Lipotoxicity reduces DDX58/Rig-1 expression and activity leading to impaired autophagy and cell death. Autophagy 18, 142–160.

Gao, J., Deng, Q., Yu, J., Wang, C., Wei, W., 2024. Role of renal tubular epithelial cells and macrophages in cisplatin-induced acute renal injury. Life Sci. 339, 122450.
Guo, Y., Che, R., Wang, P., Zhang, A., 2024. Mitochondrial dysfunction in the pathophysiology of renal diseases. Am. J. Physiol. Ren. Physiol. 326, F768–f779.
Huang, H., Han, Y., Zhang, Y., Zeng, J., He, X., Cheng, J., Wang, S., Xiong, Y., Yin, H., Yuan, Q., et al., 2025. Deletion of pyruvate carboxylase in tubular epithelial cell promotes renal fibrosis by regulating SQOR/cGAS/STING-mediated glycolysis. Adv. Sci. (Weinheim, Baden-Wurttemberg, Germany) 12, e2408753.
Imaizumi, T., Aratani, S., Nakajima, T., Carlson, M., Matsumiya, T., Tanji, K., Ookawa, K., Yoshida, H., Tsuchida, S., McIntyre, T.M., et al., 2002. Retinoic acid-inducible gene-I is induced in endothelial cells by LPS and regulates expression of COX-2. Biochem. Biophys. Res. Commun. 292, 274–279.
Islamuddin, M., Qin, X., 2024. Renal macrophages and NLRP3 inflammasomes in kidney diseases and therapeutics. Cell Death Dis. 10, 229.
Kim, J.Y., Bai, Y., Jayne, L.A., Hector, R.D., Persaud, A.K., Ong, S.S., Rojesh, S., Raj, R., Feng, M., Chung, S., et al., 2020. A kinome-wide screen identifies a CDKL5-SOX9 regulatory axis in epithelial cell death and kidney injury. Nat. Commun. 11, 1924.
Kroneisl, M., Spraakman, N.A., Koomen, J.V., Hijazi, Z., Hoogstra-Berends, F.H., Leuvenink, H.G.D., Struys, M., Henning, R.H., Nieuwenhuijs-Moeke, G.J., 2023. Peri-Operative Kinetics of Plasma Mitochondrial DNA Levels during living Donor Kidney Transplantation. Int. J. Mol. Sci. 24, 13579.
Leventoğlu, E., Bakkaloğlu, S.A., 2024. A new era in the treatment of kidney diseases: NLRP3 inflammasome and cytokine-targeted therapies. Pediatric Nephrology (Berlin, Germany) 40, 1515–1521.
Li, Y., Guo, B., 2025. GSDMD-mediated pyroptosis: molecular mechanisms, diseases and therapeutic targets. Mol. Biomed. 6, 11.
Li, Y., Xia, W., Wu, M., Yin, J., Wang, Q., Li, S., Zhang, A., Huang, S., Zhang, Y., Jia, Z., 2020. Activation of GSDMD contributes to acute kidney injury induced by cisplatin. Am. J. Physiol. Ren. Physiol. 318, F96–f106.
Li, Z., Nguyen, T.T., Valaperti, A., 2021. Human cardiac fibroblasts produce pro-inflammatory cytokines upon TLRs and RLRs stimulation. Mol. Cell. Biochem. 476, 3241–3252.
Li, N., Chen, J., Geng, C., Wang, X., Wang, Y., Sun, N., Wang, P., Han, L., Li, Z., Fan, H., et al., 2022. Myoglobin promotes macrophage polarization to M1 type and pyroptosis via the RIG-I/Caspase1/GSDMD signaling pathway in CS-AKI. Cell Death Dis. 8, 90.
Li, J.Y., Sun, X.A., Wang, X., Yang, N.H., Xie, H.Y., Guo, H.J., Lu, L., Xie, X., Zhou, L., Liu, J., et al., 2024. PGAM5 exacerbates acute renal injury by initiating mitochondria-dependent apoptosis by facilitating mitochondrial cytochrome c release. Acta Pharmacol. Sin. 45, 125–136.
Lin, Y., Luo, T., Weng, A., Huang, X., Yao, Y., Fu, Z., Li, Y., Liu, A., Li, X., Chen, D., Pan, H., 2020. Gallic Acid Alleviates Gouty Arthritis by Inhibiting NLRP3 Inflammasome Activation and Pyroptosis through Enhancing Nrf2 Signaling. Front. Immunol. 11, 580593.
Liu, C., Wei, W., Huang, Y., Fu, P., Zhang, L., Zhao, Y., 2024. Metabolic reprogramming in septic acute kidney injury: pathogenesis and therapeutic implications. Metab. Clin. Exp. 158, 155974.
Lu, H., Su, H., Liu, Y., Yin, K., Wang, D., Li, B., Wang, Y., Xing, M., 2022. NLRP3 inflammasome is involved in the mechanism of the mitigative effect of lycopene on sulfamethoxazole-induced inflammatory damage in grass carp kidneys. Fish Shellfish Immunol. 123, 348–357.
Lu, H., Guo, T., Zhang, Y., Liu, D., Hou, L., Ma, C., Xing, M., 2024. Endoplasmic reticulum stress-induced NLRP3 inflammasome activation as a novel mechanism of polystyrene microplastics (PS-MPs)-induced pulmonary inflammation in chickens. J Zhejiang Univ Sci B 25, 233–243.
Ma, L., Shen, R., Jiao, J., Lin, X., Zhai, B., Xu, A., Luo, H., Lu, L., Shao, D., 2023. Gasdermin D promotes hyperuricemia-induced renal tubular injury through RIG-I/caspase-1 pathway. iScience 26, 108463.
Maekawa, H., Inoue, T., Ouchi, H., Jao, T.M., Inoue, R., Nishi, H., Fujii, R., Ishidate, F., Tanaka, T., Tanaka, Y., et al., 2019. Mitochondrial damage Causes Inflammation via cGAS-STING Signaling in Acute Kidney Injury. Cell Rep. 29, 1261–1273 e1266.
Marchi, S., Guilbaud, E., Tait, S.W.G., Yamazaki, T., Galluzzi, L., 2023. Mitochondrial control of inflammation. Nat. Rev. Immunol. 23, 159–173.
Miao, N., Yin, F., Xie, H., Wang, Y., Xu, Y., Shen, Y., Xu, D., Yin, J., Wang, B., Zhou, Z., et al., 2019. The cleavage of gasdermin D by caspase-11 promotes tubular epithelial cell pyroptosis and urinary IL-18 excretion in acute kidney injury. Kidney Int. 96, 1105–1120.
Muñoz-Gómez, S.A., Wideman, J.G., Roger, A.J., Slamovits, C.H., 2017. The Origin of Mitochondrial Cristae from Alphaproteobacteria. Mol. Biol. Evol. 34, 943–956.
Nishimura, T., Kouwaki, T., Takashima, K., Ochi, A., Mtali, Y.S., Oshiumi, H., 2025. Cholesterol restriction primes antiviral innate immunity via SREBP1-driven noncanonical type I IFNs. EMBO Rep. 26, 560–592.
Peng, J., Wang, Y., Han, X., Zhang, C., Chen, X., Jin, Y., Yang, Z., An, Y., Zhang, J., Liu, Z., et al., 2023. Clinical Implications of a New DDX58 Pathogenic Variant that Causes Lupus Nephritis due to RIG-I Hyperactivation. J. Am. Soc. Nephrology : JASN 34, 258–272.
Poeck, H., Bscheider, M., Gross, O., Finger, K., Roth, S., Rebsamen, M., Hannesschläger, N., Schlee, M., Rothenfusser, S., Barchet, W., et al., 2010. Recognition of RNA virus by RIG-I results in activation of CARD9 and inflammasome signaling for interleukin 1 beta production. Nat. Immunol. 11, 63–69.
Pothlichet, J., Meunier, I., Davis, B.K., Ting, J.P., Skamene, E., von Messling, V., Vidal, S. M., 2013. Type I IFN triggers RIG-I/TLR3/NLRP3-dependent inflammasome activation in influenza a virus infected cells. PLoS Pathog. 9, e1003256.
Radzikowska, U., Eljaszewicz, A., Tan, G., Stocker, N., Heider, A., Westermann, P., Steiner, S., Dreher, A., Wawrzyniak, P., Rückert, B., et al., 2023. Rhinovirus-induced epithelial RIG-I inflammasome suppresses antiviral immunity and promotes inflammation in asthma and COVID-19. Nat. Commun. 14, 2329.
Rane, R.P., Soundranayagam, S., Shade, D.A., Nauer, K., DuMont, T., Nashar, K., Balaan, M.R., 2025. Renal Involvement in Sepsis: Acute Kidney Injury. Crit. Care Nurs. Q. 48, 100–108.
Ren, Q., Guo, F., Tao, S., Huang, R., Ma, L., Fu, P., 2020. Flavonoid fisetin alleviates kidney inflammation and apoptosis via inhibiting Src-mediated NF-κB p65 and MAPK signaling pathways in septic AKI mice. Biomed. Pharmacother. Biomed. Pharmacother. 122, 109772.
Seok, J.K., Yang, G., Jee, J.I., Kang, H.C., Cho, Y.Y., Lee, H.S., Lee, J.Y., 2024. Hepatocyte-specific RIG-I loss attenuates metabolic dysfunction-associated steatotic liver disease in mice via changes in mitochondrial respiration and metabolite profiles. Toxicological Res. 40, 683–695.
Shin, K.H., Lee, K.R., Kang, M.J., Chae, Y.J., 2023. Strong inhibition of organic cation transporter 2 by flavonoids and attenuation effects on cisplatin-induced cytotoxicity. Chem. Biol. Interact. 379, 110504.
Sikorska, J., Hou, Y., Chiurazzi, P., Siu, T., Baltus, G.A., Sheth, P., McLaren, D.G., Truong, Q., Parish, C.A., Wyss, D.F., 2023. Characterization of RNA driven structural changes in full length RIG-I leading to its agonism or antagonism. Nucleic Acids Res. 51, 9356–9368.
Sun, Y., Chen, X., Xie, Y., Wang, Y., Zhang, Q., Lu, Y., Li, X., 2022. TRPM7 promotes lipopolysaccharide-induced inflammatory dysfunction in renal tubular epithelial cells. Immunity. inflammation Dis. 10, e641.
Tang, R., Jin, P., Shen, C., Lin, W., Yu, L., Hu, X., Meng, T., Zhang, L., Peng, L., Xiao, X., et al., 2023. Single-cell RNA sequencing reveals the transcriptomic landscape of kidneys in patients with ischemic acute kidney injury. Chin. Med. J. 136, 1177–1187.
Thoresen, D., Wang, W., Galls, D., Guo, R., Xu, L., Pyle, A.M., 2021. The molecular mechanism of RIG-I activation and signaling. Immunol. Rev. 304, 154–168.
Wang, F., Xia, W., Liu, F., Li, J., Wang, G., Gu, J., 2012. Interferon regulator factor 1/retinoic inducible gene I (IRF1/RIG-I) axis mediates 25-hydroxycholesterol-induced interleukin-8 production in atherosclerosis. Cardiovasc. Res. 93, 190–199.
Wang, Y., Xi, W., Zhang, X., Bi, X., Liu, B., Zheng, X., Chi, X., 2022. CTSB promotes sepsis-induced acute kidney injury through activating mitochondrial apoptosis pathway. Front. Immunol. 13, 1053754.
Wicherska-Pawłowska, K., Wróbel, T., Rybka, J., 2021. Toll-like receptors (TLRs), NOD-Like receptors (NLRs), and RIG-I-Like receptors (RLRs) in innate immunity. TLRs, NLRs, and RLRs ligands as immunotherapeutic agents for hematopoietic diseases. Int. J. Mol. Sci. 22, 13397.
Yamamoto, S., Yamamoto, S., Takahashi, M., Mii, A., Okubo, A., Toriu, N., Nakagawa, S., Abe, T., Fukuma, S., Imamura, H., et al., 2024. Visualization of intracellular ATP dynamics in different nephron segments under pathophysiological conditions using the kidney slice culture system. Kidney Int. 106, 470–481.
Yao, C., Li, Z., Sun, K., Zhang, Y., Shou, S., Jin, H., 2024. Mitochondrial dysfunction in acute kidney injury. Ren. Fail. 46, 2393262.
Yu, B.C., Cho, N.J., Park, S., Kim, H., Choi, S.J., Kim, J.K., Hwang, S.D., Gil, H.W., Lee, E. Y., Jeon, J.S., et al., 2019. IgA nephropathy is associated with elevated urinary mitochondrial DNA copy numbers. Sci. Rep. 9, 16068.
Yu, J., Li, C., Ma, L., Zhai, B., Xu, A., Shao, D., 2022. Transient receptor potential canonical 6 knockdown ameliorated diabetic kidney disease by inhibiting nuclear factor of activated T cells 2 expression in glomerular mesangial cells. Ren. Fail. 44, 1780–1790.
Zhang, X., Yang, B., 2024. The serum levels of gasdermin D in uremic patients and its relationship with the prognosis: a prospective observational cohort study. Ren. Fail. 46, 2312534.
Zhang, N.N., Shen, S.H., Jiang, L.J., Zhang, W., Zhang, H.X., Sun, Y.P., Li, X.Y., Huang, Q. H., Ge, B.X., Chen, S.J., et al., 2008. RIG-I plays a critical role in negatively regulating granulocytic proliferation. Proc. Natl. Acad. Sci. USA 105, 10553–10558.
Zhang, X., Agborbesong, E., Li, X., 2021. The role of mitochondria in acute kidney injury and chronic kidney disease and its therapeutic potential. Int. J. Mol. Sci. 22.